Computer Fraud and Security
ISSN (online): 1873-7056

Impedance characteristic analysis and control strategy research of single-phase LLCL grid-connected inverter under weak grid conditions

Yanzhe Li [12*], Xun Zhu [12], Yuexin Li [1]

[1]*School of Automation & Electrical Engineering, Lanzhou Jiaotong University, Lanzhou, China*

[2] *ETAP Power System Simulation And Analysis Joint Laboratory, Lanzhou Jiaotong University, Lanzhou, China*

**Corresponding author: 503021710@qq.com*

Abstract:

Grid-connected inverters are core components for integrating clean and renewable energy technologies into the power grid and play a vital role in enhancing the stability and efficiency of the entire power system. During long-distance power transmission in grid-connected generation systems, the presence of line impedance often results in weak grid characteristics, which can trigger resonance and harmonic amplification, thereby affecting the stable operation of the grid. This paper focuses on a single-phase LLCL grid-connected inverter. First, a mathematical model of the LLCL inverter is established considering the impedance characteristics of a weak grid. By analyzing the amplitude and phase characteristics, the influence mechanism of weak grid impedance on the inverter system is revealed. The study finds that the inherent resonance peak and frequency shift of the LLCL inverter are key factors contributing to increased harmonic content in the system. To address these issues, a hybrid damping method combining active and passive damping is proposed to suppress the resonance peak. Furthermore, a composite current control strategy is designed, which parallelly integrates quasi-proportional resonant control and repetitive control, aiming to enhance the inverter's adaptability to grid frequency deviation. The results of this study provide important theoretical support for the engineering design of renewable energy grid integration and offer valuable insights into the optimization of grid-connected inverter systems.

Keywords: Grid-connected inverter; Power system; Weak grid; Line impedance; Harmonic suppression; Hybrid damping; Repetitive control; Quasi-proportional-resonant.

INTRODUCTION

New energy resources—including solar, hydropower, wind, and ocean energy—are abundant and possess significant advantages such as high efficiency, low pollution, diversification, and environmental friendliness[1]. In recent years, they have attracted increasing attention and research interest. As a key interface for integrating renewable energy into the power grid, grid-connected inverters play a crucial role in energy conversion and power quality control[2]. However, under weak grid conditions, the grid impedance exhibits significant time-variability and non-ideal characteristics, which can lead to aggravated current harmonic distortion and reduced system stability margins[3]. Therefore, investigating control strategies for single-phase LLCL-type grid-connected inverters under weak grid conditions holds substantial theoretical importance and practical relevance.

In recent years, extensive research has been conducted by scholars at home and abroad on resonance suppression and current control of inverters. In terms of resonance suppression, passive damping and active damping are the two most commonly used methods[4]. Passive damping is relatively simple to implement and low in cost, but it introduces additional power losses, thereby reducing overall system efficiency[5]. Active damping, on the other hand, incurs less power loss but requires more sensors and is more susceptible to control delays[6]. Regarding current control, Quasi-Proportional Resonant (QPR) control offers adaptability to grid frequency fluctuations, but its suppression capability for periodic harmonics is limited; repetitive control can effectively suppress periodic harmonics, yet it suffers from slower dynamic response[7].

Therefore, this paper focuses on enhancing the harmonic suppression capability of single-phase grid-connected inverter systems under weak grid conditions. The main contributions are as follows: (1) A mathematical model of the LLCL inverter under weak grid conditions is established, revealing its impedance characteristics in such scenarios; (2) A hybrid damping method combining active and passive damping is designed; (3) A composite current control strategy is proposed, which integrates QPR control with repetitive control in parallel. The innovations of this study include the novel proposal of a hybrid damping method combined with a composite

current control strategy, which enables coordinated suppression of resonance peaks and harmonic currents in inverter systems under weak grid conditions, thereby providing theoretical guidance for the current optimization strategy of grid-connected inverters.

IMPEDANCE CHARACTERISTIC ANALYSIS OF SINGLE-PHASE LLCL GRID-CONNECTED INVERTER UNDER WEAK GRID CONDITIONS

The topology of the single-phase LLCL inverter considering the impact of grid impedance under weak grid conditions is shown in Figure 1.

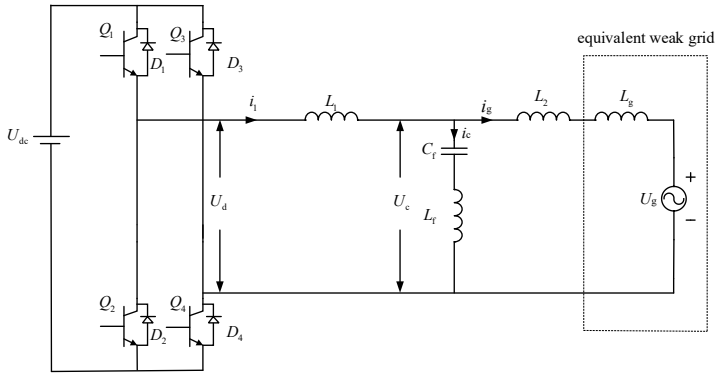

Figure 1. Topology diagram of single-phase LLCL inverter under weak grid conditions

Based on Figure 1, the control block diagram of the LLCL filter under weak grid conditions is drawn as shown in Figure 2:

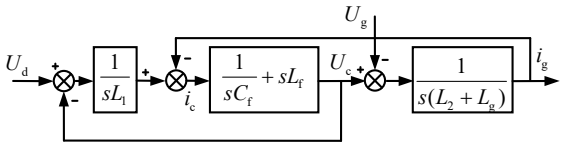

Figure 2. Control block diagram of LLCL filter under weak grid conditions

According to Figure 2, the transfer function from the inverter output voltage U_d to the grid current i_g under weak grid conditions is:

$$G_{LLCL}(s)=\frac{i_g}{U_d}=\frac{L_fC_fs^2+1}{L_1(L_2+L_g)C_fs^3+(L_1+L_2+L_g)L_fC_fs^2+(L_1+L_2+L_g)s} \quad (1)$$

To investigate the impact of grid impedance variations on the performance of the LLCL filter, the Bode plots of the LLCL filter under different grid impedance values ranging from 0 to 6 mH are drawn based on Equation (1), as shown in Figure 3.

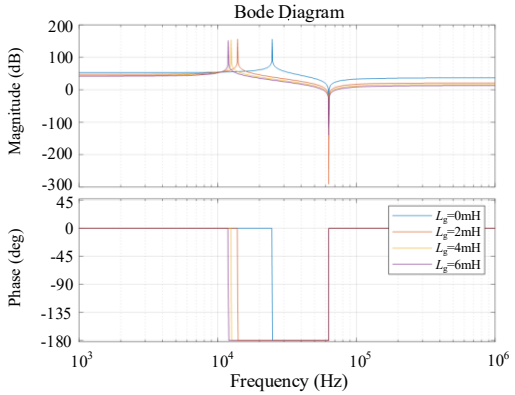

Figure 3. Bode plot of LLCL filter under different grid impedances

As analyzed from Figure 3, when the grid impedance increases, the resonance frequency of the LLCL filter gradually decreases, while the amplitude of the resonance peak remains largely unchanged. This indicates that the grid impedance primarily affects the resonance frequency, with little impact on the peak magnitude. In addition, as the grid impedance increases, the system's phase margin decreases and the bandwidth is reduced, all of which negatively affect the stability of the inverter system, leading to reduced stability.

DESIGN OF LLCL INVERTER BASED ON HYBRID DAMPING METHOD

When the inductive load introduced under weak grid conditions increases, the passive damping method leads to higher system losses and reduced efficiency due to the inclusion of physical resistors[8]. Additionally, it may weaken the harmonic attenuation capability of the LLCL filter at the switching frequency because of altered impedance characteristics. Although the active damping method avoids physical losses and has minimal impact on the filtering performance at the switching frequency, its conventional design provides limited suppression of resonance at the switching frequency and may suffer from reduced high-frequency stability due to control delays[9]. Therefore, this paper combines active and passive damping methods to adopt a hybrid damping approach. This strategy leverages the advantages of both methods, enabling the LLCL filter to maintain effective filtering and resonance suppression under weak grid conditions while adapting better to variations in grid impedance. Figure 4 shows the grid-connected inverter and its control structure based on the hybrid damping method under weak grid conditions.

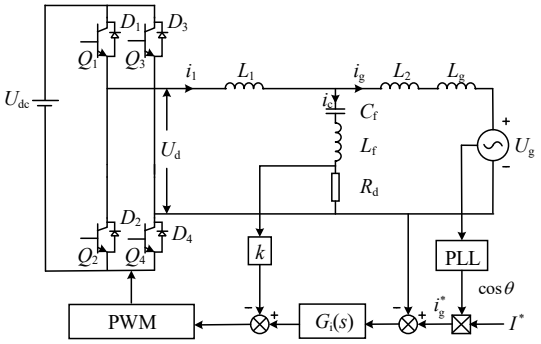

Figure 4. LLCL inverter with hybrid damping strategy and its control structure diagram

According to Figure 4, the transfer function of the mixed damping method can be obtained as follows:

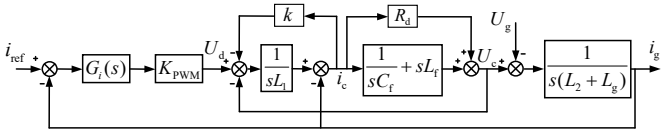

Figure 5. Structure block diagram of inverter with mixed damping method

According to Figure 5, the transfer function of the hybrid damping method can be obtained as follows:

$$G(s)=\frac{i_g(s)}{U_d(s)}=\frac{L_fC_fs^2+R_dC_fs+1}{C_f(L_1L_3+L_1L_f+L_3L_f)s^3+(R_dL_1+R_dL_3+kL_3)C_fs^2+(L_1+L_3)s} \quad (2)$$

The expressions for L_3 and k in Equation (3) are:

$$\begin{cases} L_3=L_2+L_g \\ k=\dfrac{R_d(L_1+L_3)}{L_3} \end{cases} \quad (3)$$

When analyzing the hybrid damping method, the value of resistor R_d is a very important part, the size of Rd not only affects the stability and filtering performance of the system under the weak grid, but also affects the additional loss of the system. the larger R_d is, the lower the gain at the resonant frequency of the system, the better the suppression of the resonance spikes, but the harmonic suppression at the switching frequency becomes worse. In

order to make the system maintain good harmonic suppression ability at the switching frequency while suppressing the resonance spikes at the resonance frequency and switching frequency, this paper selects R_d= 1Ω, which makes the system have better filtering performance while avoiding larger power loss.

In order to study the performance of the LLCL filter with hybrid damping method under weak grid conditions, the Bode diagram of the LLCL filter with hybrid damping method is plotted according to Equation 2 when the grid impedance varies from 0 to 6 mH, as shown in Figure 6.

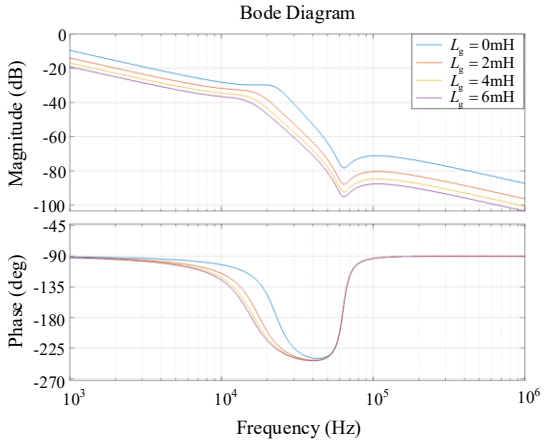

Figure 6. Bode diagram of hybrid damping with different values of L_g

Comparison of Figure 6 with Figure 3 shows that the resonance peaks of the system are well suppressed when the grid impedance is 0mH, 2mH, 4mH, and 6mH, respectively, and the amplitude difference between the different L_g counterpart curves is small, and the overall trend of the phase curves is flat, without any local violent jumps, which indicates that the hybrid damping method suppresses the resonance spikes to a certain extent under the weak grid condition and improves the robustness of the LLCL filter to the changes in grid impedance, but the resonance frequency shift is not completely suppressed. robustness of the LLCL filter to grid impedance changes, but the resonant frequency shift is not completely suppressed.

Therefore, to address the shortcomings of the hybrid damping method, this paper designs a composite current control strategy with QPR control and improved repetition control in parallel to reduce the effect of line impedance on the stability of the grid-connected inverter.

COMPOUND CONTROL STRATEGY

The QPR controller relaxes the strict tracking requirement of the resonant frequency on the basis of the traditional PR control by introducing ω_c, which improves the adaptability and robustness of the system to the fluctuation of the grid frequency[10].The transfer function of the QPR control is:

$$G_{QPR} = K_p + \frac{2K_r\omega_c s}{s^2 + 2\omega_c s + \omega_0^2} \qquad (4)$$

Where, ω_0 is the fundamental angular frequency and its value is 314 rad/s; ω_c is the bandwidth coefficient, which directly affects the system bandwidth and gain distribution, and ω_c=5 rad/s is adopted in this paper. K_p mainly affects the gain at the non-fundamental frequency of the QPR controller. The larger the value of K_p, the better the immunity of the system, but the greater the impact on the stability of the system. In this paper, K_p=10. The value of K_r must take into account the gain at the fundamental frequency and the stability of the system. In this paper, K_r=400.

The Bode diagram of the QPR controller based on Equation 4 is shown in Figure 7. An analysis of Figure 7 shows that the QPR control bandwidth is large, expanding the resonant peak into a frequency band of finite width, so that the controller can still maintain a high gain in a certain range near the resonant frequency. In a weak grid with large grid frequency fluctuations, the wide bandwidth characteristic of QPR can maintain sufficient gain near the offset frequency, thus better adapting to the grid frequency fluctuations and resonant frequency offset, effectively suppressing the new harmonic components, reducing the adverse effects of the weak grid on the system, and

avoiding the control performance degradation caused by frequency mismatch in conventional PR. However, the QPR control still suffers from the problem of residual steady state error in suppressing periodic noncharacteristic subharmonic components, especially when the grid background harmonics exhibit multi-frequency repetitive characteristics. In this paper, the repetitive control is introduced into the QPR control to construct a composite controller, which realizes the full-period tracking and elimination of the full-band harmonics.

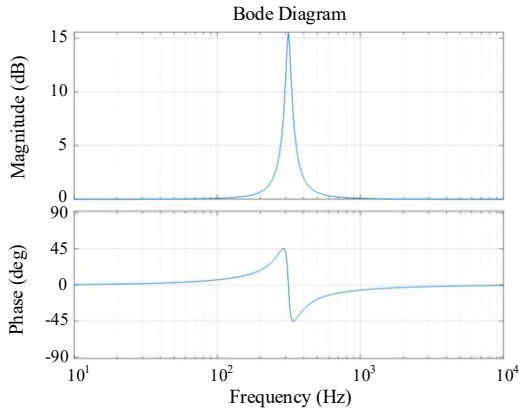

Figure 7. QPR controller bode diagram

The core idea of repetitive control is based on the internal model principle, the core structure of which is to achieve complete tracking and suppression of periodic interference or reference signals by embedding an internal model in the controller that generates periodic signals[11]. Figure 8(a) shows the internal model structure of the ideal repetition controller. The poles of the ideal repeating internal model are located on the imaginary axis (corresponding to the unit circle in the discrete domain), which leads to a critical stable state of the system, and a slight parameter fluctuation may cause instability[12]. Therefore, it is necessary to improve the standard internal model, and the improved internal model is shown in Figure 8(b).

(a) Improved front inner mold (b) Improved internal mold

Figure 8. Internal model structure diagram

The block diagram of the improved repetitive control structure is shown in Figure 9, where $P(z)$ is the discrete form of the controlled object, $S(z)$ is the compensation link, and $d(z)$ is the external disturbance.

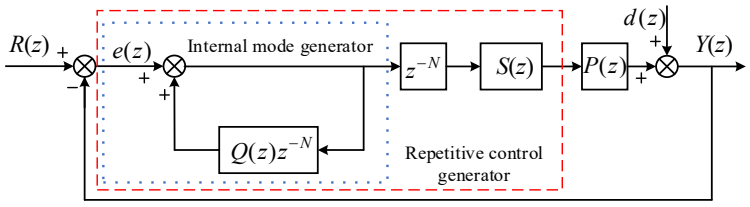

Figure 9. Improved repetitive control structure block diagram

In the compensation step $S(z)=k_r z^k C_1(z)C_2(z)$, k_r is the repetitive control gain, and the amplitude of the signal is compensated. z^k is the lead link, which is used to compensate the phase lag caused by $P(z)C(z)$, $C(z)= C_1(z)C_2(z)$, $C_1(z)$ is a second-order filter, and $C_2(z)$ is a zero-phase shift trap. $S(z)$ needs to be designed according to the controlled object.

According to the above analysis, QPR control has high gain at the fundamental frequency, can effectively track the fundamental frequency signal, and is suitable for dealing with dynamic processes such as power grid frequency fluctuations and load mutations, but its ability to suppress periodic interference is limited. Repetitive control has

significant advantages in tracking and suppressing periodic signals, but the dynamic response is slow, and it is difficult to quickly deal with dynamic processes such as frequency fluctuations or load mutations[13]. Therefore, based on the hybrid damping method, this paper proposes a compound control scheme that parallel QPR control and improved repetitive control, so that the inverter system can maintain stable operation when the grid impedance changes under the condition of weak power grid, and reduce the influence of transient process when the grid frequency fluctuations, so that the system has a good dynamic response. Its basic structure is shown in Figure 10.

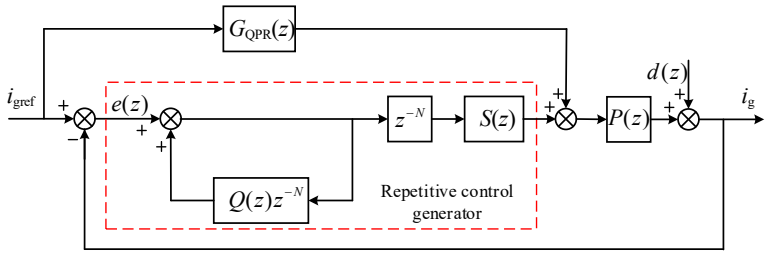

Figure 10. Composite control structure block diagram

The closed-loop transfer function of the composite system is:

$$G(z)=\frac{P(z)\left[G_{QPR}(z)+G_{RC}(z)\right]}{1+P(z)\left[G_{QPR}(z)+G_{RC}(z)\right]} \qquad (5)$$

The closed-loop system characteristic polynomial can be obtained from Equation 5 as:

$$\begin{aligned}1+\left[G_{QPR}(z)+G_{RC}(z)\right]P(z)&=1+G_{QPR}(z)P(z)+G_{RC}(z)P(z)\\&=\left[1+G_{QPR}(z)P(z)\right]\left[1+\frac{G_{RC}(z)P(z)}{1+G_{QPR}(z)P(z)}\right]\\&=\left[1+G_{QPR}(z)P(z)\right]\left[1+G_{RC}(z)P_0(z)\right]\\&=\Delta_1\Delta_2\end{aligned} \qquad (6)$$

Where $P_0(z)$ is the equivalent control object for repetitive control.

$$P_0(z)=\frac{P(z)}{1+G_{QPR}(z)P(z)} \quad (7)$$

For a stable discrete system, it is necessary to make the roots of Δ_1 and Δ_2 in Equation 7 both within the unit circle. The characteristic root of $\Delta_1=0$ is in the unit circle, that is, the system is stable when the QPR controller acts alone, and the characteristic root of $\Delta_2=0$ is in the unit circle, that is, to ensure that the equivalent control object $P_0(z)$ is stable when the repetitive controller acts alone. The stability condition of the system can be obtained as follows:

$$\left|Q(z)z^{-N}\left[1-z^k k_r C(z)P_0(z)\right]\right|<1(\forall z=e^{sT}=e^{j\omega T},0<\omega<\pi/T) \qquad (8)$$

When the frequency signal is an integer multiple of the base wave:

$$z^{-N}=1 \quad (9)$$

Substituting Equation 9 into Equation 8 yields:

$$\left|1-z^k k_r C(z)P_0(z)\right|<1 \qquad (10)$$

Based on amplitude-frequency characteristics:

$$C(j\omega)=N_C(\omega)e^{-j\theta_C(\omega)} \qquad (11)$$

$$P_0(j\omega)=N_P(\omega)e^{-j\theta_P(\omega)} \qquad (12)$$

Substituting Equation 11 and Equation 12 into Equation 10 yields:

$$\left|1-k_{\mathrm{r}}N_{\mathrm{C}}(\omega)N_{\mathrm{P}}(\omega)e^{-j[\theta_{\mathrm{C}}(\omega)+\theta_{\mathrm{P}}(\omega)]+k\omega}\right|<1 \qquad (13)$$

According to Euler's formula:

$$e^{-j[\theta_{\mathrm{C}}(\omega)+\theta_{\mathrm{P}}(\omega)]+k\omega}=\cos\left[\theta_{\mathrm{C}}(\omega)+\theta_{\mathrm{P}}(\omega)+k\omega\right]-j\sin\left[\theta_{\mathrm{C}}(\omega)+\theta_{\mathrm{P}}(\omega)+k\omega\right] \qquad (14)$$

Seek out:

$$\left|\theta_{\mathrm{C}}(\omega)+\theta_{\mathrm{P}}(\omega)+k\omega\right|<90° \qquad (15)$$

$$0<k_{\mathrm{r}}<\min_{\omega}\frac{2\cos\left[\theta_{\mathrm{C}}(\omega)+\theta_{\mathrm{P}}(\omega)+k\omega\right]}{N_{\mathrm{C}}(\omega)N_{\mathrm{P}}(\omega)} \qquad (16)$$

Thus the system is stabilized when the parameters k and k_{r} satisfy Equation 15 and Equation 16, respectively.

Next, the parameters of each section of the improved repetition controller will be designed so that it meets the system stability requirements.

Where N is the sampling frequency within a fundamental wave period, take the system sampling frequency f_{s} = 10kHz, fundamental wave frequency f_0 = 50Hz, then $N = f_{\mathrm{s}}/f_0$=200. In order to achieve good stability and simplify the repetitive controller design, $Q(z)$ is a constant less than 1, $Q(z)$=0.95.

According to Equation (1), when the system adopts hybrid damping method, the resonant peak value corresponds to ω=1.22×10^4 rad/s. In order to attenuate the resonance peak at this frequency, the design of the compensation link in this paper adopts the method of combining low-pass filter and notch. Considering that the amplitude-frequency characteristics of the second-order filter will fluctuate and introduce significant phase lag when it attenuates high-frequency harmonics, it is necessary to accurately calculate its natural frequency ω_{n}. The calculation formula is as follows:

$$\omega_{\mathrm{n}}=\omega\sqrt{1-2\xi^2+\sqrt{4\xi^4-4\xi^2+2}} \qquad (17)$$

$$C_1(s)=\frac{\omega_{\mathrm{n}}^2}{s^2+2\xi\omega_{\mathrm{n}}s+\omega_{\mathrm{n}}^2} \qquad (18)$$

In the equation, ξ is the damping ratio. In order to ensure the system has good transient response performance, ξ= 0.8 is selected and substituted into the Equation (17) to obtain ω_{n}=1.06×10^4 rad/s. Substituting ω_{n} into Equation (18) and discretizing with ZOH(order 0 holder), we can get:

$$C_1(z)=\frac{0.3163z+0.1781}{z^2-0.6891z+0.1831} \qquad (19)$$

The basic form of a zero phase shift trap is:

$$C_2(z)=\frac{z^m+2+z^{-m}}{4} \qquad (20)$$

In the frequency domain, $z = \mathrm{e}^{j\omega T_{\mathrm{s}}}$, $\theta = \omega T_{\mathrm{s}}$, plug into the Equation (20) to get:

$$C_2(\theta)=\frac{e^{jm\theta}+2+e^{-jm\theta}}{4}=\frac{\cos m\theta+1}{2} \qquad (21)$$

m affects the trap frequency, and there are multiple trap frequencies. From Equation (21), it can be obtained:

$$m=\frac{\pi}{\omega T_{\mathrm{s}}} \qquad (22)$$

Substituting ω=1.22×10^4 rad/s, T_{s}=1/f_{s} into the Equation (22) gives m=2.55, rounding m≈3, so:

$$C_2(z)=\frac{z^3+2+z^{-3}}{4} \qquad (23)$$

The lead link z^k is used to compensate the phase lag caused by $P(z)C(z)$. When k takes different values, the phase frequency characteristic curve of $P(z)C(z)$ is shown in Figure 11.

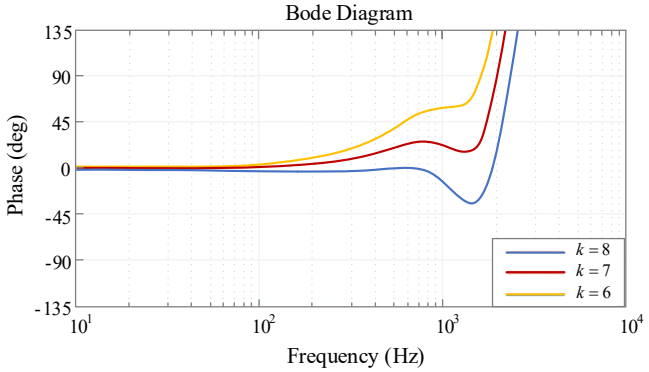

Figure 11. Phase frequency curve of $P(z)C(z)$ for different k values

When k=7, $P(z)C(z)$ is closer in the middle and low frequency bands, so z^7 is chosen in this paper.

The control gain coefficient k_r is a constant design parameter with a range of values satisfying $k_r \leq 1$. The main function of this parameter is to adjust the compensation strength of the repetition controller. When k_r is taken to its maximum value of 1, the system is able to realize the optimal tracking performance of the reference signal, but the stability and anti-interference ability of the system will be reduced accordingly[14]. In order to select a suitable value of k_r, it is defined according to Equation (10):

$$H(e^{j\omega})=\left|Q(z)[1-z^k k_r C(z)P_0(z)]\right| \qquad (24)$$

Where $z = e^{j\omega}$.

At this point Equation (10) can be changed to $H(e^{j\omega})<1$, that is, the end of the vector $H(e^{j\omega})$ is in the unit circle and the system is stable. Since $H(e^{j\omega})<1$ is the stability criterion for the whole system, it is necessary to consider the system computational delay z^{-1}, such that:

$$P_1(z)=P_0(z)z^{-1} \quad (25)$$

Then the stability criterion becomes:

$$H_1(e^{j\omega})=\left|Q(z)[1-z^k k_r C(z)P_1(z)]\right| \qquad (26)$$

According to Equation 26, the Nyquist plots of $H_1(e^{j\omega})$ are plotted in Figure 12 for k_r 0.6, 0.7, 0.8, and 0.9, respectively.

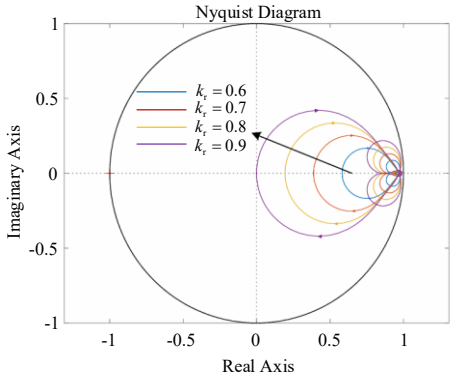

Figure 12. Nyquist diagram of $H_1(e^{j\omega})$ for different values of k_r

Analysis of the curve shows that increasing the repetitive control gain k_r can accelerate the error convergence process and enhance the harmonic suppression effect, but at the same time, it will lead to a decrease in the stability margin of the system. In order to realize the optimal coordination between the system stability and the tracking accuracy of the command signal, k_r =0.8 is chosen.

SIMULATION ANALYSIS

According to Figure 4, the simulation model of a single-phase LLCL grid-connected inverter was built in Matlab/Simulink to verify the effectiveness of the control strategy proposed in this paper under weak power grid conditions.

Figure 13 shows the simulation waveform of the grid-connected current. It can be observed that the grid-connected current tracks the reference current command exceptionally well, with a near-zero phase difference between them, and the waveform is smooth and distortion-free. Figure 14 presents the FFT analysis of the grid-connected current. The results demonstrate low high-frequency harmonic content at the switching frequency, attributed to the effective attenuation of switching-frequency harmonics by the hybrid damping method. The THD of the grid-connected current is only 1.12%, significantly lower than the 5% limit specified in the IEEE 1547 standard. This confirms that the proposed composite control strategy exhibits excellent low-frequency harmonic suppression capability and fully complies with the power quality requirements for grid connection.

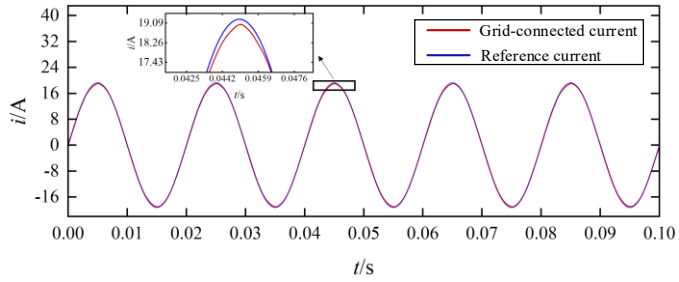

Figure 13. Simulation waveform of grid-connected current and reference current

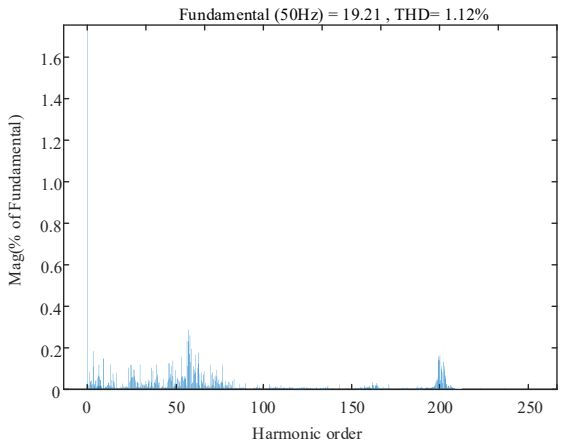

Figure 14. FFT diagram of grid-connected current

Since the repetitive control has a slow dynamic response and is not suitable to be used alone, the grid-connected currents under composite control and QPR control are mainly compared in the simulation to highlight the combined effect of the combination of QPR and repetitive control. Figure 15 and Figure 16 show the simulated waveforms and FFT plots of the grid-connected current under the QPR control strategy, respectively. Through the comparison study with Figure 13 and Figure 14, it is concluded that under the weak grid condition, the grid-connected current under single QPR control has poor tracking ability to the reference current, with distortion of sinusoidal waveforms, and the THD value reaches 1.57%; whereas, after adopting the composite control strategy of QPR+repeat control, it is able to output a better sinusoidal waveform, and the THD reduces by 0.45%, which fully proves that the composite control strategy has a significant role in The superiority of the composite control strategy in improving current tracking accuracy and suppressing harmonics effectively overcomes the

performance defects of the single control method.

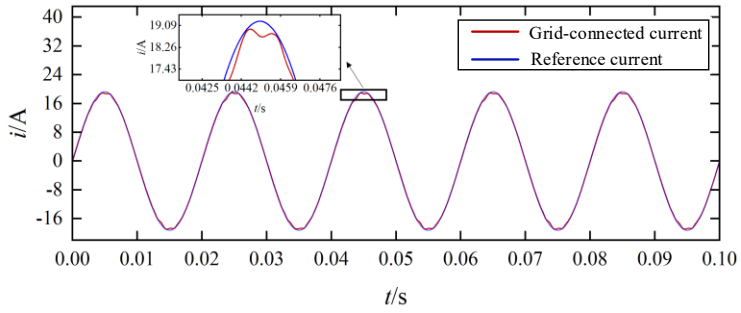

Figure 15. Simulated waveforms of grid-connected current with QPR control

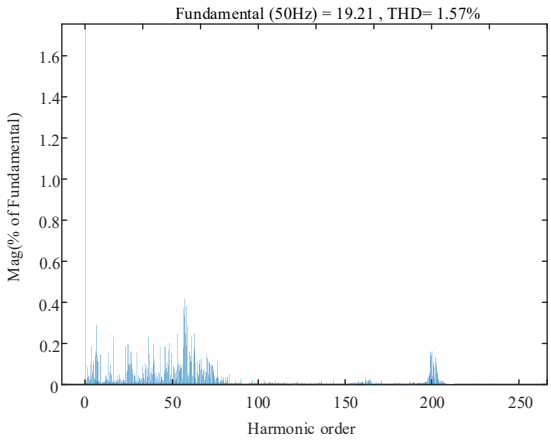

Figure 16. FFT diagram of grid-connected current with QPR control

To verify the robustness of the proposed control strategy, simulations were conducted with circuit impedance values of 3mH and 6mH, as shown in figure 17 and figure 18, respectively. By comparing the results with the reference waveform under ideal grid conditions (0mH grid impedance, as shown in Figure 13), it can be observed that the grid-connected current maintains good sinusoidal quality even with increased grid impedance, without serious waveform distortion or phase shift. The simulation results demonstrate that the control strategy designed in this paper effectively mitigates the impact of impedance under weak grid conditions, ensuring stable system operation and maintaining high-quality power output.

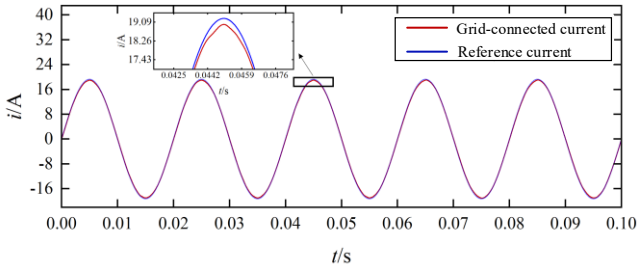

Figure 17. Grid-connected current simulation waveform with L_g=3mH

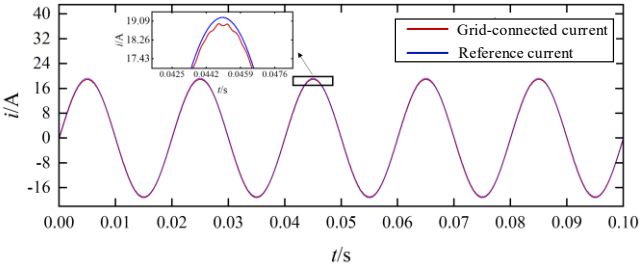

Figure 18. Grid-connected current simulation waveform with L_g=6mH

CONCLUSION

In this paper, the influence mechanism of impedance characteristics on the stability of single-phase LLCL grid-connected inverters under weak grid conditions is systematically investigated, and the mathematical model of single-phase LLCL inverter under weak grid conditions is established, which reveals that grid impedance mainly affects the stability of the inverter system by changing the resonance frequency. The stable operation of the LLCL inverter under weak grid conditions is realized by the cooperative control of hybrid damping method and composite control strategy, which suppresses the resonance spikes and improves the filtering capability of the inverter. Simulation results show that the adopted control strategy keeps the grid-connected current with better current quality under different grid impedances, and the THD value is reduced by 0.45% compared with the pre-improvement period, which verifies the effectiveness of the strategy. The research results provide theoretical support for the design of the grid-connected inverter, which provides an important reference value for new energy access to the grid. In the future, the adaptive parameter regulation mechanism can be further explored, combined with model predictive control or intelligent optimization algorithms, to improve the inverter's dynamic regulation capability and anti-interference performance under the complex grid environment.

REFRENCES

[1] Peng Wenbiao, Liu Junfeng, Zhang Yanjun, et al. New energy evaluation based on natural resource attributes: A case study of hunan province[J]. Sustainable Development, 2022, 12(4):117-128.

[2] Yang Z, Yang F, Min H, et al. Review on optimal planning of new power systems with distributed generations and electric vehicles[J]. Energy Reports, 2023, 9: 501-509.

[3] Zhuo C, Xin J, Hong H, et al. Review on impedance modeling of grid-connected inverters under weak grid conditions[J]. Integrated Intelligent Energy, 2024, 46(6): 88–101.

[4] Meng L, Wang C, Guerrero J M. Comparative analysis of passive and active damping methods for LLC resonant converters in photovoltaic systems[J]. Renewable Energy, 2021, 178: 1249-1261.

[5] Guo X Q, Wu W. Modeling and stability analysis of direct output current control for grid-connected inverters with LCL interface[J]. Transactions of China Electrotechnical Society, 2010, 25(3): 102-109.

[6] Li Z J, Yang J R, Liu H J, et al. A grid-side active damping strategy to enhance the passivity of grid-connected inverters under a weak grid[J]. Grid and Clean Energy, 2024, 40(06): 145-154.

[7] Chen G M, Xu L L. Adaptive quasi-proportional resonant control with parameter estimation for PMSM sensorless control[J]. Advances in Mechanical Engineering, 2023, 15(2): 1–13.

[8] Wang X, Li Y, Xu D. Passive damping design for LCL filters in grid-connected inverters considering parameter variations[J]. IEEE Transactions on Industrial Electronics, 2021, 68(7): 5678-5689.

[9] Zhong X, Wang Y, Wang Y, et al. Active damping method based self-adjust notch filter for current source converter[J]. The Journal of Engineering, 2019, 2019(17): 4165–4170.

[10] Zijie F, Junfeng L, Hao Z, et al. Disturbance observer-based quasi-proportional resonant composite control strategy for high-frequency LCLC inverters[J]. International Journal of Circuit Theory and Applications, 2023, 51(10): 4711–4727.

[11] Brandão Jr O da S, Pereira L F A, Flores J V. A systematic method for repetitive controller design based on the process frequency response[J]. Journal of Control, Automation and Electrical Systems, 2022, 33(6): 1364–1374.

[12] Althobaiti A, Ullah N, Belkhier Y, et al. Expert knowledge based proportional resonant controller for three phase inverter under abnormal grid conditions[J]. International Journal of Green Energy, 2023, 20(7): 767–783.

[13] Zhang Y, Zhou J, Han X, et al. Adaptive odd repetitive control for magnetically suspended rotor harmonic currents suppression[J]. Journal of Vibration and Control, 2023, 29(9–10): 1115–1128.

[14] Jia C, Longman R W, Dong E. Low-order sliding mode repetitive control for discrete-time systems under complex disturbance environment[J]. International Journal of Robust and Nonlinear Control, 2021, 31(11): 5188–5217.